## Magnetization hysteresis and time decay measurements in ${ m FeSe}_{0.50}{ m Te}_{0.50}$ : Evidence for fluctuation in mean free path induced pinning

P. Das<sup>1,2\*</sup>, Ajay D. Thakur<sup>1†</sup>, Anil K. Yadav<sup>1</sup>, C. V. Tomy<sup>1</sup>, M.R. Lees<sup>3</sup>, G. Balakrishnan<sup>3</sup>, S. Ramakrishnan<sup>2</sup>, A. K. Grover<sup>2</sup>

<sup>1</sup> Department of Physics, Indian Institute of Technology Bombay, Mumbai 400076, India

 $^2\ DCMP \&MS,\ Tata\ Institute\ of\ Fundamental\ Research,$ 

Homi Bhabha Road, Colaba, Mumbai 400005, India

<sup>3</sup> Department of Physics, University of Warwick, Coventry CV4 7AL, UK

(Dated: March 7, 2019)

## Abstract

We have explored the vortex phase diagram in a single crystal of  $FeSe_{0.5}Te_{0.50}$  with a  $T_c=14.3$  K via detailed magnetization measurements. The possible role of the crystalline anisotropy on vortex pinning is explored via magnetic torque magnetometry. We present evidence in favor of pinning related to spatial variations of the charge carrier mean free path leading to small bundle vortex pinning by randomly distributed (weak) pinning centers. The dynamical response across second magnetization peak (SMP) anomaly in  $FeSe_{0.5}Te_{0.50}$  has been compared with that across the well researched phenomenon of peak effect (PE) in a single crystal of  $CeRu_2$ .

PACS numbers: 74.25.Qt, 74.78.Na, 74.78.Db, 74.25.Fy, 73.23.-b, 73.50.-h

<sup>\*</sup> Present Address: Institute of Materials Science, The University of Tsukuba, 1-1-1, Tennodai, Ibaraki 305-8573, Japan

<sup>†</sup> Corresponding Author Email: ajay@phy.iitb.ac.in

The discovery of superconductivity in quaternary (1111) Iron (Fe) pnictide system LaFeAsOF at 26 K [1] opened the flood gates for explorations on Fe based superconducting systems. Vigorous research in related systems has already demonstrated the existence of superconductivity in several Fe-based compounds including the ThCr<sub>2</sub>Si<sub>2</sub>-tructure based quaternary  $(Ba, Sr)_{1-x}K_xFe_2As_2$  (122) [2], the ternary LiFeAs (111) [3] and the binary FeSe/Te (11) [4]. In an uncanny resemblance to the importance of Cu-O planes in the cuprate high  $T_c$ superconductors, the FeAs or, FeSe/Te layers play a vital role in Fe-based superconductors. Amongst them the tetragonal FeSe/Te system has proved to be promising to understand the basic mechanism of superconductivity in Fe-based materials. The Fermi surface of the tetragonal system is very similar to that reported for the FeAs based superconductors [5], comprising cylindrical electron sections at the zone corners, cylindrical hole surface sections, and small hole sections at the zone center. Furthermore, these surfaces are separated by a 2D nesting vector at  $(\pi, \pi)$ , another characteristic reminiscent of the FeAs based superconductors. Despite an apparent structural simplicity of FeSe/Te vis a vis other Fe-based systems, its physics is already shown to be both rich as well as interestingly complex. There have been reports hinting towards the possibility of an anisotropy in the symmetry of order parameter [6], multiple band gaps [7] and a dominant Pauli paramagnetic effect in the upper critical field(s)  $(H_{c2})$  [8]. Also, the high pressure studies have shown an enhancement in T<sub>c</sub> to as high as 36 K in the FeSe system at a pressure of 38 GPa [9, 10]. In view of the promising fabrication of superconducting wires of FeSe/Te by powder-in-tube technique [11], it becomes important to understand its vortex phase diagram and the pinning mechanism. Prozorov et al. [12] have reported the dynamical response of the flux line lattice via isothermal M-H scans and magnetic relaxation measurements in Ba(Fe<sub>0.93</sub>Co<sub>0.07</sub>)<sub>2</sub>As<sub>2</sub> and found a crossover from the collective to plastic creep regime near the peak position of the fishtail feature. Yadav et al [13, 14] have reported magnetic and transport studies in FeTe<sub>0.6</sub>Se<sub>0.4</sub> which has an optimal  $T_c$  in the FeSe/Te system. It is indeed of interest to explore vortex physics in samples with a smaller  $T_c$  (away from optimal composition). Discovery of still higher  $T_c \sim 30~K$  in  $\mathrm{K}_{0.8}\mathrm{Fe}_2\mathrm{Se}_2$  [15] and proposals for enhancing  $T_c$  via suitable substitution in excess at the Fe site [16] have made vortex state studies on FeSe based systems all the more desirable. Magnetic relaxation studies are warranted to explore the pinning mechanism as well as its possible connection to crystalline anisotropy. Relaxation studies have been performed in the past on a host of low-T<sub>c</sub> and high-T<sub>c</sub> superconducting materials. In this paper we report detailed magnetization measurements on FeSe<sub>0.50</sub>Te<sub>0.50</sub> superconductor with a  $T_c = 14.3$  K. This includes: (i) observation of the second magnetization peak (SMP) (i.e., a fishtail feature), (ii) calculation of crystalline anisotropy based on torque magnetometry measurements, (iii) the estimation of flux pinning force density  $(F_p)$ , (iv) obtaining the vortex phase diagram, and (v) magnetic relaxation across SMP. Based on the above results, we try to provide an understanding of the underlying pinning mechanisms and compare and contrast with our earlier results in the well studied CeRu<sub>2</sub> system [17].

The FeSe<sub>0.5</sub>Te<sub>0.5</sub> single crystal used for the present work was grown using the modified Bridgeman method. For the magnetization measurements we chose a parallelepiped shaped piece weighing 22.5 mg. The crystal has T<sub>c</sub> of 14.3 K. The DC magnetization studies were performed using PPMS-VSM and SQUID-VSM, Quantum Design Inc., (USA) for field applied both parallel and perpendicular to the c-axis. The scan amplitude was chosen to be 2.0 mm and 1.0 mm for the PPMS-VSM and SQUID-VSM, respectively. Torque magnetometry measurements were performed on the sample using a suitably calibrated torque lever chip on a PPMS Tq-MAG (Quantum Design Inc., USA) option.

The panel (a) of Fig.1 shows typical five quadrant isothermal magnetization hysteresis (M-H) loops recorded at several temperatures between 5 K and 14 K and for  $H \parallel c$ . The minimum in magnetization located at a field value little above nominal zero field in a given M-H loop represents the first magnetization peak characteristic which amounts to (near) full penetration of the applied field in the bulk of the sample after zero field cooling. Thereafter, a prominent SMP, also known as the fishtail effect (FE), can be observed in the M-H data at 7 K, 9 K and 11 K. The onset  $(H_{\rm SMP}^{\rm on})$  and peak  $(H_{\rm SMP}^{\rm p})$  positions of SMP are marked for the 7 K plot. Both  $H_{\text{SMP}}^{\text{on}}$  and  $H_{SMP}^{p}$  are seen to decrease along with the hysteresis width as the temperature enhances from 5 K towards 12 K. At 14 K, M-H loop, on repeated cycling, has a shape akin to that in a magnetically ordered system. However the onset of diamagnetic response, pertaining to the onset of superconductivity can be identified by using the deviation of linearity criterion (from the paramagnetic normal state response), while decreasing the field from above the upper critical field  $(H_{c2})$  [18]. We could determine  $H_{c1}$  values from the virgin portion (after zero field cooling) of the M-H curves (up to 12.5) K), using the deviation of linearity criterion from the Meissner response. In panel (b) of Fig.1, we present the M-H loops recorded at several temperatures for  $H \perp c$ . The scenario here is quite different when compared to the situation for  $H \parallel c$ . Here, we do not observe a clear signature of SMP within our measurement range of field values. This essentially suggests an anisotropy in the pinning behavior of the flux line lattice. Another significant observation is that the magnetization on the return leg is not a mirror image of the M-H response on the forward leg. The decrease in magnetization on reducing the field reflects the significant "magnetic contribution" to the M-H, which is distinct from the hysteresis response originating from the macroscopic super currents set up in the sample. However, a careful look at return leg of the M-H loop at 11 K seems to suggest the presence of SMP like characteristic for  $H \perp c$  as well.

There are distinct differences in the observed scenario in the cases for fields parallel and perpendicular to the c-axis, respectively from the perspective of the observation of SMP. This leads to the issue of the possible role of crystalline anisotropy and its effect on the vortex lattice structures. A direct way to experimentally obtain the anisotropy parameter  $\gamma$  (=  $\frac{H_{cb}^{2b}}{H_{c2}^c} = \frac{\xi_{ab}}{\xi_c} = \frac{\lambda_c}{\lambda_{ab}} = \frac{m_c^*}{m_{ab}^*}$  for a conventional, single-band, s-wave superconductor) is via measuring the torque acting on a superconducting sample in the mixed state with the magnetic field being applied at various angles with respect to the crystalline axis. We performed torque magnetometry measurements on our single crystal of FeSe<sub>0.50</sub>Te<sub>0.50</sub>. Figure 2 shows the torque ( $\tau(\theta)$ ) data obtained at a temperature of 11 K at 5 kOe. In the field range  $H_{c1} \ll H \ll H_{c2}$ , the torque density is given by,  $\tau = \frac{\phi_0 B(\gamma^2 - 1) \sin 2\theta}{64\pi^2 \lambda^2 \gamma^{1/3} \varepsilon(\theta)} ln \frac{\eta H_{c2,a}}{\varepsilon(\theta)}$  [19, 20]. Here,  $\theta$  is the angle between the magnetic induction B and the crystalline c-axis,  $\varepsilon(\theta) = \sqrt{\sin^2 \theta + \gamma^2 \cos^2 \theta}$ ,  $\lambda^3 = \lambda_a^2 \lambda_c$  and  $\eta \sim 1$ . The torque data is fitted using the above equation yielding an anisotropy parameter of 3.17.

We may extract critical current density values from the isothermal M-H data making use of the Bean's critical state model formalism [21], where,  $J_c = 20 \frac{\Delta M}{a(1-\frac{a}{3b})}$  [22], with 'a' and 'b' being the sample dimensions perpendicular to the field direction, and  $\Delta M$  is the difference between the magnetization measured during the return and the forward legs of the M-H loop. The main panel in Fig. 3 shows the plot of the normalized critical current density  $J_c^{norm}(H)$  at the temperatures of 5 K, 7 K, 9 K and 11 K. Here, the normalization has been done with the  $J_c$  value at the peak position of SMP (where the correlation volume of the vortex lattice is expected to attain a minimum value [18]). In the case of the 9 K data,  $H_{\rm SMP}^{\rm on}$  and  $H_{\rm SMP}^{\rm p}$  are marked by arrows. The inset in Fig.3 shows a color scale contour plot of  $J_c(H,t)$ , where  $t=\frac{T}{T_c}$  is the reduced temperature.

In order to understand the nature of pinning in more detail, it is useful to look at the

variation of pinning force density,  $F_p$  with magnetic field. In Fig. 4, we show the plot of normalized pinning force density  $(F_p^{norm})$  as a function of reduced magnetic fields h  $(=H/H_{irr})$ , where,  $H_{irr}$  is the field at which  $J_c$  is measurably zero) at 10 K and 11 K. Here, the reduced field is obtained by normalizing the applied field with respect to the field value at which the observed  $J_c$  is measurably small (denoted by the irreversibility field  $H_{irr}$ , as the magnetic response is reversible beyond this field). Note that the  $F_p^{norm}$  curves for the two temperature values collapse into a unified curve. We fit this data within the Dew-Hughes scenario  $(F_p \sim h^{\alpha}(1-h)^{\beta})$  [23, 24]. The Dew-Hughes fit is shown by the dark black line in Fig.4 and it yields the following values of the exponents: (a)  $\alpha = 1.688 \pm 0.006$ , and (b)  $\beta = 2.363 \pm 0.008$ . In the case of a system dominated by point pinning alone,  $\alpha = 1$ and  $\beta = 2$  with  $F_p^{max}$  occurring at  $h_{max} \approx 0.33$ . In contrast, grain boundary pinning is expected to lead to  $h_{max} \approx 0.2$ , whereas, pinning due to variations in the order parameter leads to  $h_{max} \approx 0.7$  [23, 24]. In our case,  $F_p^{max} \approx 0.42$ , implying that point pins alone can not rationalize the observed scenario. In the case of BaFe<sub>1.8</sub>Co<sub>0.2</sub>As<sub>2</sub>,  $h_{max} \approx 0.33$ suggesting a possible correlation with inhomogeneous distribution of Co ions [25]. Similarly, Kim et al [26] attributed  $h_{max} \approx 0.33$  in  $Ba_{0.68}K_{0.32}Fe_2As_2$  to arsenic deficiency. Sun et al [27] did a similar analysis for a number of electron doped and hole doped iron-arsenide based superconductors, which included  $Ba_{0.68}K_{0.32}Fe_2As_2$  ( $h_{max} \approx 0.43$ ),  $BaFe_{1.85}Co_{0.15}As_2$  $(h_{max} \approx 0.37)$  and BaFe<sub>1.91</sub>Ni<sub>0.09</sub>As<sub>2</sub>  $(h_{max} \approx 0.33)$ . They observed that H<sub>c2</sub> and H<sub>SMP</sub> decreased faster with decreasing temperatures for the Ni-substituted sample than for the Ksubstituted or the Co-substituted samples. Their observation was corroborated by the larger  $\Delta T_c$  for the Ni-substituted sample. However, the K-substituted sample showed the strongest pinning amongst the three systems, suggesting that an inhomogeneous distribution of dopant can not by itself explain the strong pinning in iron-arsenide based superconductors. Magnetic decoration experiments by Vinnikov et al [28] in a variety of iron arsenide superconductors showed a disordered vortex state whose nature was seen to be independent of the crystal structure type, doping and synthesis methods. The absence of an Abrikosov vortex lattice upto field values of 200 Oe in their experiments suggests the dominance of small bundle pinning in these classes of superconductors. The intrinsic mechanism of pinning in these materials however remains intriguing [29, 30].

Nature of pinning in type-II superconductors can be broadly classified into two categories: (i) the one arising because of the spatial fluctuations in the transition temperature,  $T_c$  (known as  $\delta T_{\rm c}$  pinning) across the sample, and (ii) the one caused by the spatial variations in the charge carrier mean free path, l (known as  $\delta l$  pinning). In the case of  $\delta T_{\rm c}$  pinning, the normalized critical current density,  $J_{\rm c}(t)/J_{\rm c}(0)=(1-t^2)^{7/6}(1+t^2)^{5/6}$  while for  $\delta l$  pinning,  $J_{\rm c}(t)/J_{\rm c}(0)=(1-t^2)^{5/2}(1+t^2)^{-1/2}$ , where  $t=T/T_{\rm c}$  [31, 32]. In Fig. 5, we plot the normalized  $J_{\rm c}(t)$  data at 5 kOe (open stars) and 10 kOe (open circles). These have been extracted from the  $J_{\rm c}(H)$  plots at various reduced temperature values  $t(=\frac{T}{T_{\rm c}})$ . The theoretical estimates of  $J_{\rm c}(t)/J_{\rm c}(0)$  within the scenarios of  $\delta T_{\rm c}$  pinning and  $\delta l$  pinning are shown by bold lines. The observations point to the dominance of the  $\delta l$  pinning mechanism in FeSe<sub>0.50</sub>Te<sub>0.50</sub>, suggesting the occurrence of single vortex pinning by randomly distributed weak pinning centers.

In Fig. 6, we plot the vortex phase diagram for the case  $H \parallel c$ . The locations of  $H_{\rm SMP}^{\rm on}$ ,  $H_{\rm SMP}^{\rm p}$ ,  $H_{\rm irr}$  and  $H_{c2}$  (as obtained via isothermal M-H measurements) are shown by filled square, filled circle, open circle and open diamond symbols, respectively. Accordingly, the vortex phase diagram is divided into several phases comprising of (i) the Bragg Glass phase, (ii) the multi-domain vortex glass phase (where, dislocation lines permeate the vortex lattice however, there is non-vanishing long range spatial correlations between vortices), (iii) the pinned amorphous phase (where, there are no long range spatial correlations between the vortices however,  $J_c$  is still non-zero due to small bundle pinning), and (iv) the quasivortex liquid phase (where, there are no spatial correlations between the vortices and  $J_c$  is nearly zero). The locus of  $H_{\rm SMP}^{\rm on}$ ,  $H_{\rm SMP}^{\rm p}$  are fitted using the expressions  $H_{\rm SMP}^{\rm on}(T) = H_{\rm SMP}^{\rm on}(0) \left(1 - \frac{T}{T_c}\right)^{1.3}$  and  $H_{\rm SMP}^{\rm p}(T) = H_{\rm SMP}^{\rm p}(0) \left(1 - \frac{T}{T_c}\right)^{1.5}$ , respectively. The least square fits yield  $H_{\rm SMP}^{\rm on}(0) = 17.45~kOe$  and  $H_{\rm SMP}^{\rm p}(0) = 123.8~kOe$ . Similar power-law behavior for the onset and peak fields for SMP were observed in the cases of YBCO [33] and Ba<sub>0.6</sub>K<sub>0.4</sub>Fe<sub>2</sub>As<sub>2</sub> [34].

Our observation of a dominant  $\delta l$  pinning in FeSe<sub>0.50</sub>Te<sub>0.50</sub> is in contrast to a recent claim of a prevalent  $\delta T_{\rm c}$  pinning in FeSe<sub>0.40</sub>Te<sub>0.60</sub> by Liu et al [35]. It should however be noted that the temperature dependence of the  $H_{\rm SMP}^{\rm on}$  and  $H_{SMP}^{p}$  lines (see Fig. 6) are similar to those reported for YBCO [33], whose pinning properties were seen to be dominated by the  $\delta l$  pinning mechanism [32]. Also in their report, Liu et al [35] have not attempted to make a quantification of the temperature variation of normalized critical current density, they attribute the broadening of the SMP as a signature of  $\delta T_{\rm c}$  pinning.

Exploring vortex dynamics in FeSe based superconductors has the potential of shedding

some additional light on the pinning behavior and occurrence of order-disorder transformation in its vortex matter. Peak effect (PE) and SMP are well researched attributes associated with phase transformations in vortex matter. While the former is seen to occur close to the H<sub>c2</sub> (T) line in the vortex matter phase diagram, the latter is observed deep within the mixed state [36]. Both are associated with a concominant increase in the vortex pinning energy and hence an anomalous modulation in  $J_c$ . Changes in dynamical time scales across these characteristics are anticipated and are seen to occur in a wide variety of experiments in low  $T_c$  and high  $T_c$  superconductors [37–40]. Taking cue from such observations, we attempt to make a similar analysis across the SMP in our single crystal of FeSe<sub>0.50</sub>Te<sub>0.50</sub> and compare it with that in a single crystal of another low  $T_c$  superconductor CeRu<sub>2</sub> ( $T_c \approx 8 K$ ), which displays only the PE phenomenon [38]. In particular, the normalized magnetic relaxation rate, S, given by  $S = \left| \frac{dlnM}{dlnt} \right|$ , estimates the thermally activated flux creep involving different types of barriers for several models central to the understanding of vortex dynamics. Panel (a) of Fig. 7 shows a portion of the two quadrant isothermal M-H loop at 9 K for FeSe<sub>0.5</sub>Te<sub>0.5</sub> single crystal. The inset in Fig. 7 (a) shows the time decay (M(t)) data at 27 kOe and 9 K (measured up to 10<sup>4</sup> s). The magnetization values at 10<sup>4</sup> s for various field values along the return leg are shown by open red symbols (with dotted red line as a guide to eye for the portion of the time evolved M-H loop at 10<sup>4</sup> s). Figure 7 (b) shows a plot of S(H) at 9 K across SMP for the same sample. Modulation in S appears to have little correlation with the modulation of M across SMP. Figure 8 (a) shows a portion of the M-H loop for CeRu<sub>2</sub> in the peak effect (PE) region at 4.5 K. The inset in Fig. 8 (b) shows the complete two quadrant isothermal M-H loop at the same temperature. Note that there is current decay across the PE region, and the filled square data points show the M values after an interval of 1000 s. The dotted line is a guide to eye for a section of the decayed PE loop. The inset shows a typical M(t) profile at 20 kOe. In Fig. 8 (b), we show a plot of S(H) across the PE region in CeRu<sub>2</sub>. There is a non-monotonic modulation in S across PE. Following observations are worth noting: (i) The M-H loop is reversible (no hysteresis) over a considerable field range (5 kOe to 19 kOe at 4.5 K) prior to the onset of PE  $(H_{PE}^{on})$  in CeRu<sub>2</sub> (see inset in Fig. 8(b)). In this region,  $J_c$  is nearly zero with no measurable time evolution. Consequently, S is essentially zero in this region (see Fig. 8(b)). In contrast,  $J_c$  is non-zero prior to the onset of SMP  $(H_{SMP}^{on})$  in FeSe<sub>0.5</sub>Te<sub>0.5</sub>, there is a significant time decay response and consequently, the baseline value of S is non-zero prior to  $H_{SMP}^{on}$ . (ii) S varies non-monotonically across both the SMP in FeSe<sub>0.5</sub>Te<sub>0.5</sub> as well as across the PE in CeRu<sub>2</sub>, (iii) The field values for the maxima in S do not exactly coincide with  $H_{SMP}^p$  (or,  $H_{PE}^p$ ). However, it is worthwhile to note that the ballpark field region (between  $H_{PE}^{on}$  and  $H_{PE}^p$ ) where, S peaks in the case of CeRu<sub>2</sub>, coincides with the field value at which a jump in equilibrium magnetization across PE in CeRu<sub>2</sub> was observed by Tulapurkar *et al* [41].

The PE in CeRu<sub>2</sub> is associated with an order-disorder transition. The occurrence of SMP in weakly pinned type-II superconductors has also been conjured as a manifestation of a disorder driven order-disorder transition. In a typical field ramp experiment, vortices are injected into the sample through inhomogeneous surface barriers leading to the formation of transient disordered vortex states (TDVS) within the sample [39, 40]. Here, it is interesting to understand the non-monotonic modulation in S in FeSe<sub>0.50</sub>Te<sub>0.50</sub> within the picture of annealing of these TDVS across the order-disorder phase transition in vortex lattices. Kalisky et al [39] reported the role of TDVS on the magnetic relaxation across the SMP in single crystals of Bi2212. The non-monotonicity of S with H across the SMP is evident in their observations. The observation of a similar non-monotonic variation of S across SMP in our single crystal of FeSe<sub>0.50</sub>Te<sub>0.50</sub> fortifies the plausibility of the occurrence of a similar order-disorder transformation. Closeness in the numerical values of S across the SMP in FeSe<sub>0.50</sub>Te<sub>0.50</sub> and that across PE in CeRu<sub>2</sub> could also point to similarity in the nature of current decay across SMP and PE features, however, a more conclusive inference can not be arrived at from our present data.

To summarize, we have explored the phenomenon of SMP across (H, T) vortex phase diagram in FeSe<sub>0.40</sub>Te<sub>0.60</sub>. There are considerable differences in the observed scenario in the cases for fields parallel and perpendicular to the c-axis, respectively. This in turn suggests the possible role of crystalline anisotropy and its effect on the vortex lattice structures. A possible role of magnetocrystalline anisotropy on the occurence of SMP is explored via torque magnetometry and we obtain a value of 3.17 for  $\gamma$ . Attempt is made to quantify the observations within the Dew-Hughes scenario [23, 24]. Such an analysis appears to suggest that point pins alone can not rationalize the observed field variation of the pinning force density. A comparison of the observed  $J_c(t)$  values is made with the anticipated temperature variations within the  $\delta l$  and  $\delta T_c$  pinning scenarios. We find strong evidence for  $\delta l$  pinning leading to small bundle vortex pinning by randomly distributed weak pinning centers. Experimental signatures via magnetic relaxation studies suggesting the possibility

of an order-disorder transformation across SMP is seen in the case of FeSe<sub>0.50</sub>Te<sub>0.50</sub> and a comparison with the case of PE phenomenon in CeRu<sub>2</sub> is drawn. The observations presents a strong case for a dedicated local probe measurement (either via magneto-optical imaging or, by a suitable magnetic decoration technique) which is expected to shed more light on the finer details of the pinning mechanism in Fe-based superconductors.

We would like to thank Prof. Y. Onuki for providing the single crystal of CeRu<sub>2</sub>. CVT and GB wishes to acknowledge financial support for this research from EPSRC, UK. CVT would like to acknowledge the Department of Science and Technology for partial support through the project IR/S2/PU-10/2006. AKY would like to thank CSIR, India for SRF grant. ADT acknowledges the Institute Post-Doctoral Fellowship at the Indian Institute of Technology for partial support.

Y.Kamihara, H.Hiramtsu, M.Hirano, R.Kawamura, H.Yanagi, T. Kamiya, and H.Hosono; J.
 Am. Chem. Soc. 128, 10012 (2006); *ibid* 130, 3296 (2008).

<sup>[2]</sup> M. Rotter, M. Tegel, D. Johrendt, Phys Rev. Lett. 101 026403 (2008).

<sup>[3]</sup> J. H. Tapp, Z. Tang, B. Liv, K. Sasmal, B. Loerez, P. C. W. Chu and A. M. Guloy, Phys Rev B 78, 060505 (2008).

<sup>[4]</sup> F. C. Hsu, J. Y. Luo, K. W. Yeh, T. K. Chen, T. W. Huang, P. M. Wu, Y. C. Lee, Y. L. Huang, Y. Y. Chu, D.C. Yan, and M.K. Wu, Proc. Natl. Acad. Sci. (USA) 105, 14262 (2008).

<sup>[5]</sup> A. Subedi, L. Zhang, D. J. Singh, and M. H. Du, Phys. Rev. B 78, 134514 (2008).

<sup>[6]</sup> R. Khasanov, K. Conder, E. Pomjakushina, A. Amato, C. Baines, Z. Bukowsaki, J. Karpinski, S. Katrych, H.H. Klauss, H. Luetkens, A. Shengelaya, and N.D. Zhigadlo, Phys Rev B 78, 220510(R) (2008).

<sup>[7]</sup> H. Kotegawa, S. Masaki, Y. Awai, H. Tou, Y. Mizuguchi, and Y. Takano, J. Phys. Soc. Jpn. 77, 113703 (2008).

<sup>[8]</sup> Seunghyun Khim, Jae Wook Kim, Eun Sang Choi, Yunkyu Bang, Minoru Nohara, Hidenori Takagi and Kee Hoon Kim, arXiv: 1001.4017.

<sup>[9]</sup> S. Medvedev, T.M. McQueen, I. Trojan, T. Palasyuk, M.I. Eremets, R.J. Cava, S. Naghavi, F. Casper, V. Ksenofontov, G. Wortmann, C. Felser, Nature Materials 8, 630 (2009).

<sup>[10]</sup> S. Margadonna, Y. Takabayashi, Y. Ohishi, Y. Mizuguchi, Y. Takano, T. Kagayama, T.

- Nakagawa, M. Takata, K. Prassides, Phys. Rev. B 80, 064506 (2009).
- [11] T. Ozaki, K. Deguchi, Y. Mizuguchi, Y. Kawasaki, T. Tanaka, T. Yamaguchi, H. Kumakura, and Y. Takano, arXiv: 1103.3602.
- [12] R. Prozorov et al., Phys. Rev. B 78, 224506 (2008).
- [13] C S Yadav, P L Paulose, New Journal of Physics 11, 103046 (2009).
- [14] C. S. Yadav, P. L. Paulose, arXiv:1002.0248.
- [15] J. Guo, S. Jin, G. Wang, S. Wang, K. Zhu, T. Zhou, M. He, X. Chen, Phys. Rev. B 82, 180520 (2010).
- [16] A. K. Yadav, A. D. Thakur, C. V. Tomy, Sol. St. Comm. 151, 557 (2011).
- [17] D. Pal, A. D. Thakur, D. Jaiswal, S. Ramakrishnan, A.K. Grover, E. Yamamoto, Y. Haga, M. Hedo, Y. Inada and Y. Onuki, Sol. St. Phys. (India) 46, 623 (2003).
- [18] D. Jaiswal-Nagar, A. D. Thakur, S. Ramakrishnan, A. K. Grover, D. Pal, and H. Takeya, Phys. Rev. B 74, 184514 (2006).
- [19] V. G. Kogan, Phys. Rev. B 38, 7049 (1988).
- [20] D. E. Farrel, C. M. Williams, S. A. Wolf, N. P. Bansal, and V. G. Kogan, Phys. Rev. Let t. 61, 2805 (1988).
- [21] C. P. Bean, Rev. Mod. Phys. 36, 31 (1964).
- [22] C. P. Poole Jr., H. A. Farach, R. J. Creswick, R. Prozorov, Superconductivity, Second edition (2007), Academic Press.
- [23] D. Dew-Hughes, Philos. Mag. 30, 293 (1974).
- [24] A. M. Campbell, J. E. Evetts and D. Dew-Hughes, Philos. Mag. 18, 313 (1968).
- [25] A. Yamamoto, J. Jaroszynski, C. Tarantini, L. Balicas, J. Jiang, A. Gurevich, D. C. Larbalestier, R. Jin, A. S. Sefat, M. A. McGuire, B. C. Sales, D. K. Christen, and D. Mandrus, Appl. Phys. Lett. 94, 062511 (2009).
- [26] H.-J. Kim, Y. Liu, Y. S. Oh, S. H. Khim, I. Kim, G. R. Stewart, and K. H. Kim, Phys. Rev. B 79, 014514 (2009).
- [27] D. L. Sun, Y. Liu, and C. T. Lin, Phys. Rev. B 80, 144515 (2009).
- [28] L. Ya. Vinnikov, T. M. Artemova, I. S. Veshchunov, N. D. Zhigadlo, J. Karpinski, P. Popovich, D. L. Sun, C. T. Lin, and A. V. Boris, JETP Lett. 90, 299 (2009).
- [29] D. S. Inosov et al., Phys. Rev. B 81, 014513 (2010).
- [30] M. R. Eskildsen et al., Phys. Rev. B 79, 100501(R) (2009).

- [31] G. Blatter, M. V. Feigel'man, V. B. Geshkenbein, A. I. Larkin, and V. M. Vinokur, Rev. Mod. Phys. 66, 1125 (1994).
- [32] R. Greissen, W. Hai-hu, A. J. J. van Dalen, B. Dam, J. Rector, H. G. Schnack, S. Libbrecht, E. Osquiguil, and Y. Bruynseraede, Phys. Rev. Lett. 72, 1910 (1994).
- [33] L. Klein, E. R. Yacoby, Y. Yeshurun, A. Erb, G. Muller-Voigt, V. Breit, H. Wuhl, Phys. Rev. B 49, 4403 (1994).
- [34] H. Yang, H. Luo, Z. Wang, and H-H Wen, Appl. Phys. Lett. 93, 142506 (2008).
- [35] Y. Liu, K. Kremer, and C. T. Liu, Euro. Phys. Lett. 92, 57004 (2010).
- [36] S. Sarkar, D. Pal, P. L. Paulose, S. Ramakrishnan, A. K. Grover, C. V. Tomy, D. Dasgupta, Bimal K. Sarma, G. Balakrishnan, and D. McK. Paul, Phys. Rev. B 64, 144510 (2001).
- [37] Y. Yeshurun, A. P. Malozemoff, and A. Shaulov, Rev. Mod. Phys. 68, 911 (1996) and references therein.
- [38] P. C. Ho, S. Moehlecke, and M. B. Maple, cond-mat: 0301281.
- [39] B. Kalisky, Y. Bruckental, A. Shaulov, and Y. Yeshurun, Phys. Rev. B 73, 014501 (2006).
- [40] A.D. Thakur, D. Pal, M.J. Higgins, S. Ramakrishnan, and A.K. Grover, Physica C 466, 181 (2007); ibid 460, 1259 (2007).
- [41] A. A. Tulapurkar, D. Heidarian, S. Sarkar, S. Ramakrishnan, A.K. Grover, E. Yamamoto, Y. Haga, M. Hedo, Y. Inada and Y. Onuki, Physica C 355, 59 (2001).

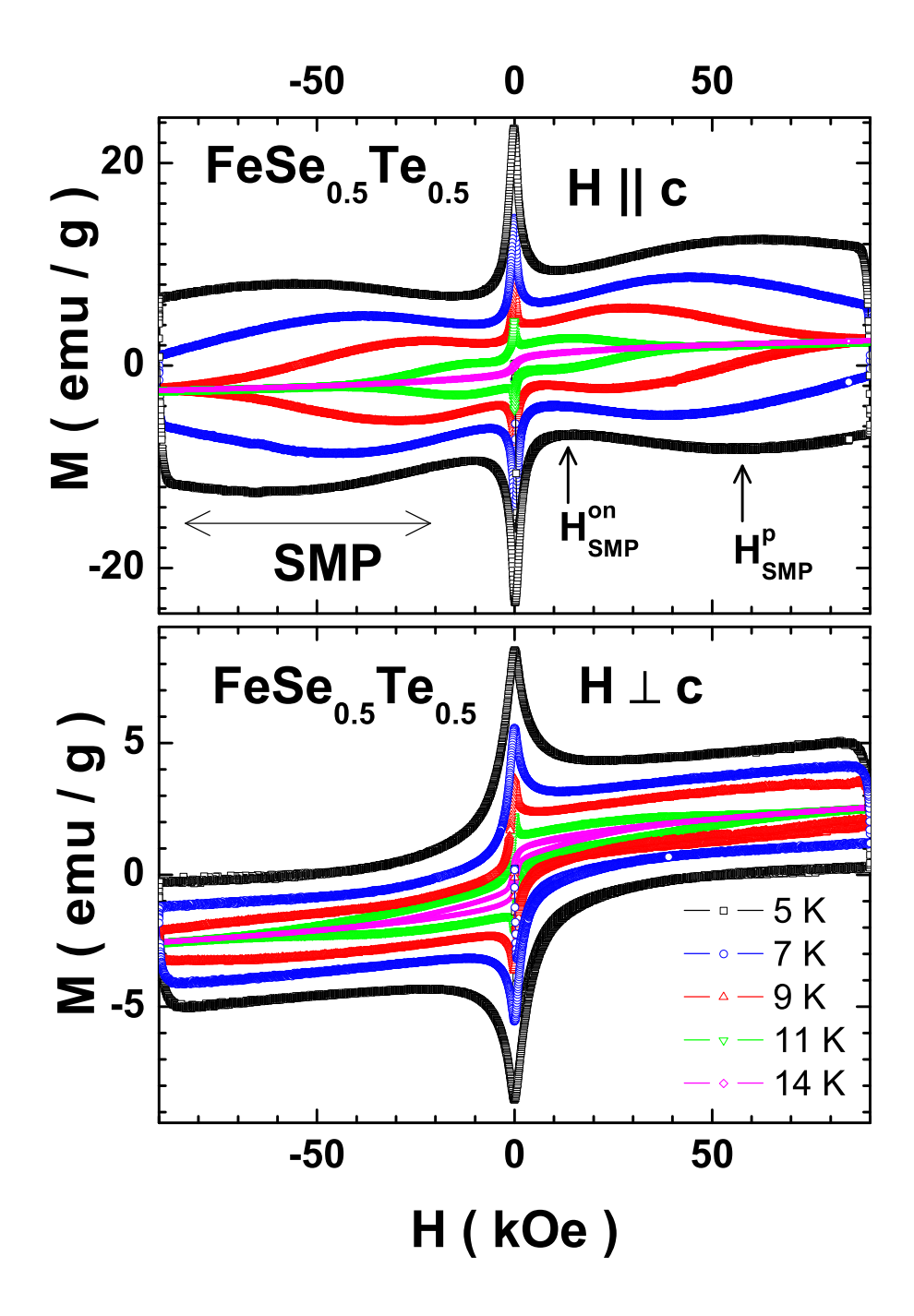


FIG. 1: (Color online) Isothermal M-H measurements in a single crystal of FeSe<sub>0.50</sub>Te<sub>0.50</sub> at various temperatures as indicated for the case of: (a)  $H \parallel c$ , and (b)  $H \perp c$ .

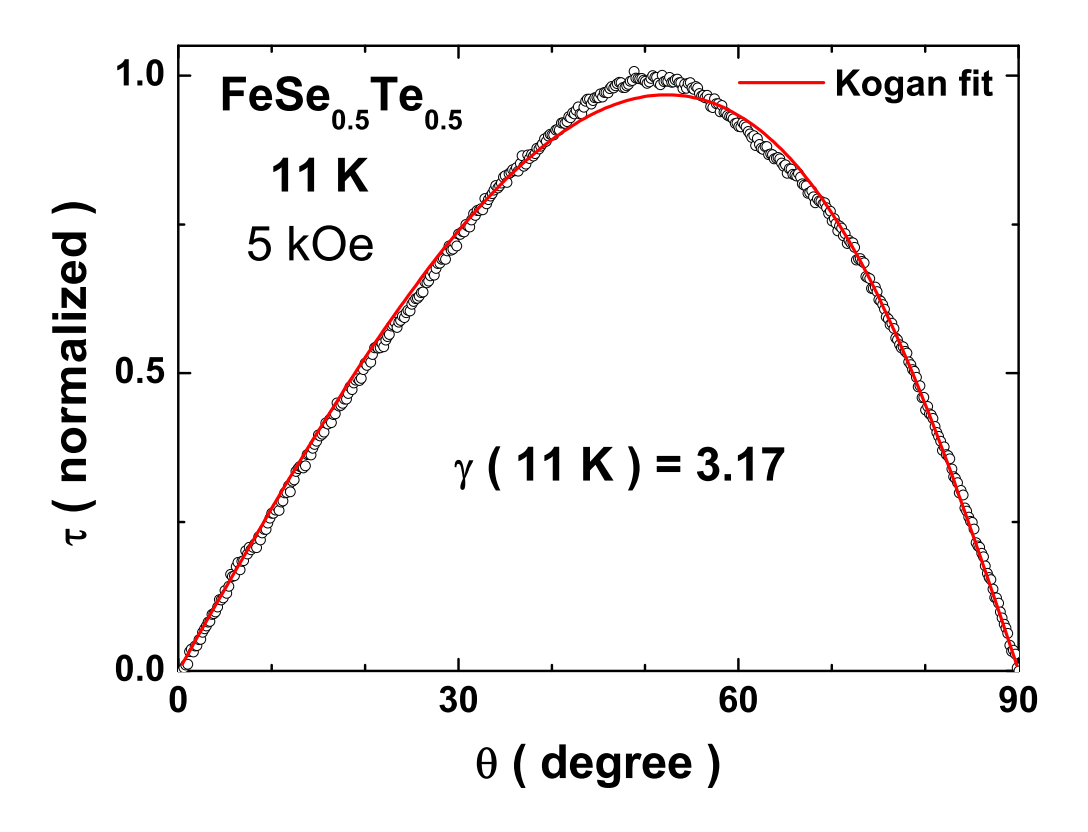


FIG. 2: (Color online) Torque magnetometry data (see text) as a function of  $\theta$  in a single crystal of FeSe<sub>0.50</sub>Te<sub>0.50</sub> at 11 K and 5 kOe. The black solid line shows the fit to the Kogan equation [19, 20].

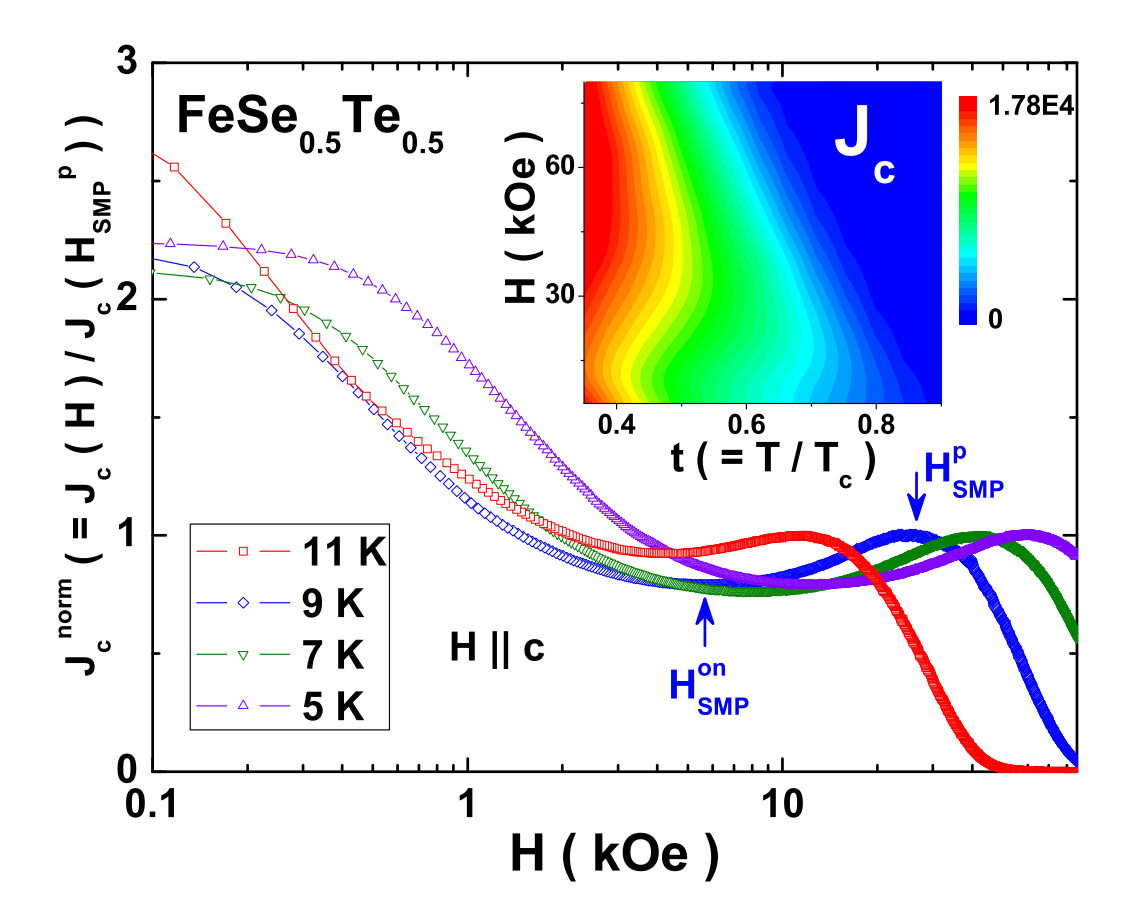


FIG. 3: (Color online)  $J_c^{norm}(H)$  (=  $J_c(H)/J_c(H_{\rm SMP}^p)$  in a single crystal of FeSe<sub>0.50</sub>Te<sub>0.50</sub> at different temperatures, as indicated. Inset shows a color scale plot of the critical current density,  $J_c(H, t)$ , where t (=  $T/T_c$ ) is the reduced temperature. The characteristics of SMP can be clearly seen for reduced temperature values in the interval 0.35 < t < 0.50.

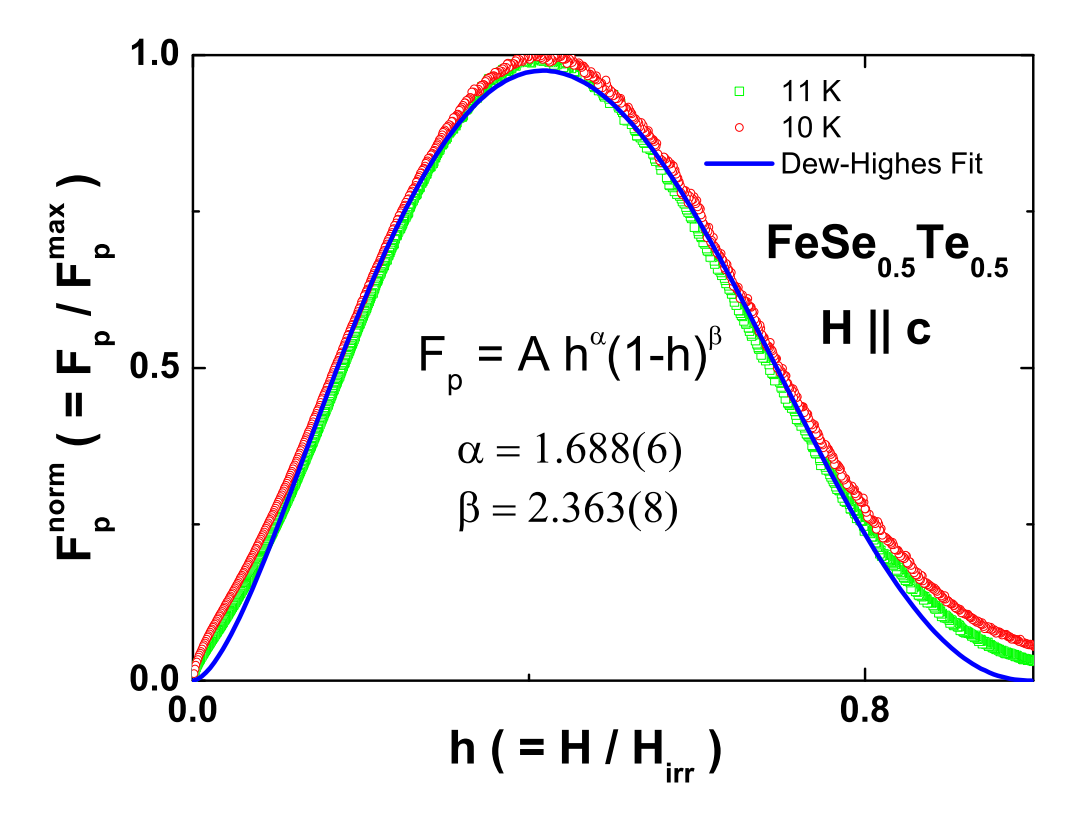


FIG. 4: (Color online) Normalized pinning force density,  $F_p^{norm}$  (=  $F_p(H)/F_p^{max}(H)$  as a function of reduced field, h (=  $H/H_{irr}$ ). The solid red line shows the fit to the Dew-Hughes's formula  $F_p \sim h^{\alpha} (1-h)^{\beta}$ .

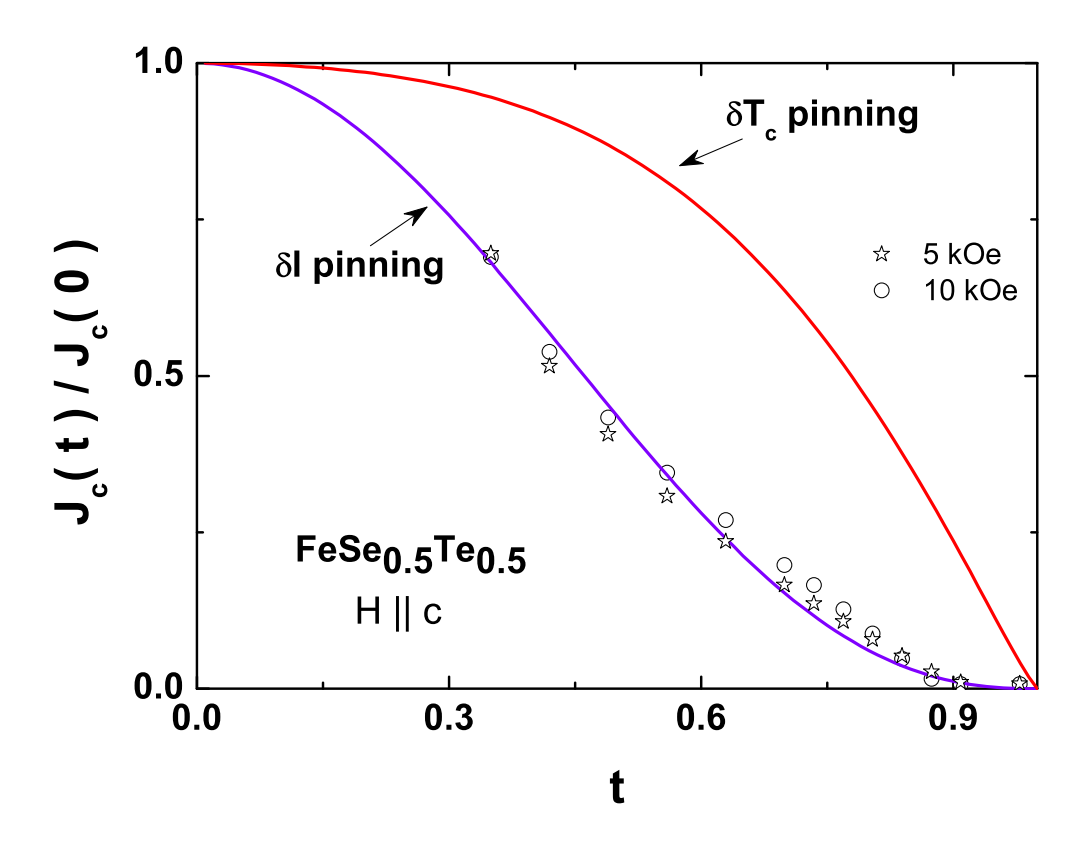


FIG. 5: (Color online) Normalized  $J_{\rm c}(t)$  data at 5 kOe (open stars) and 10 kOe (open circles). The theoretical estimates for  $\delta T_{\rm c}$  and  $\delta l$  pinning are shown by bold lines.

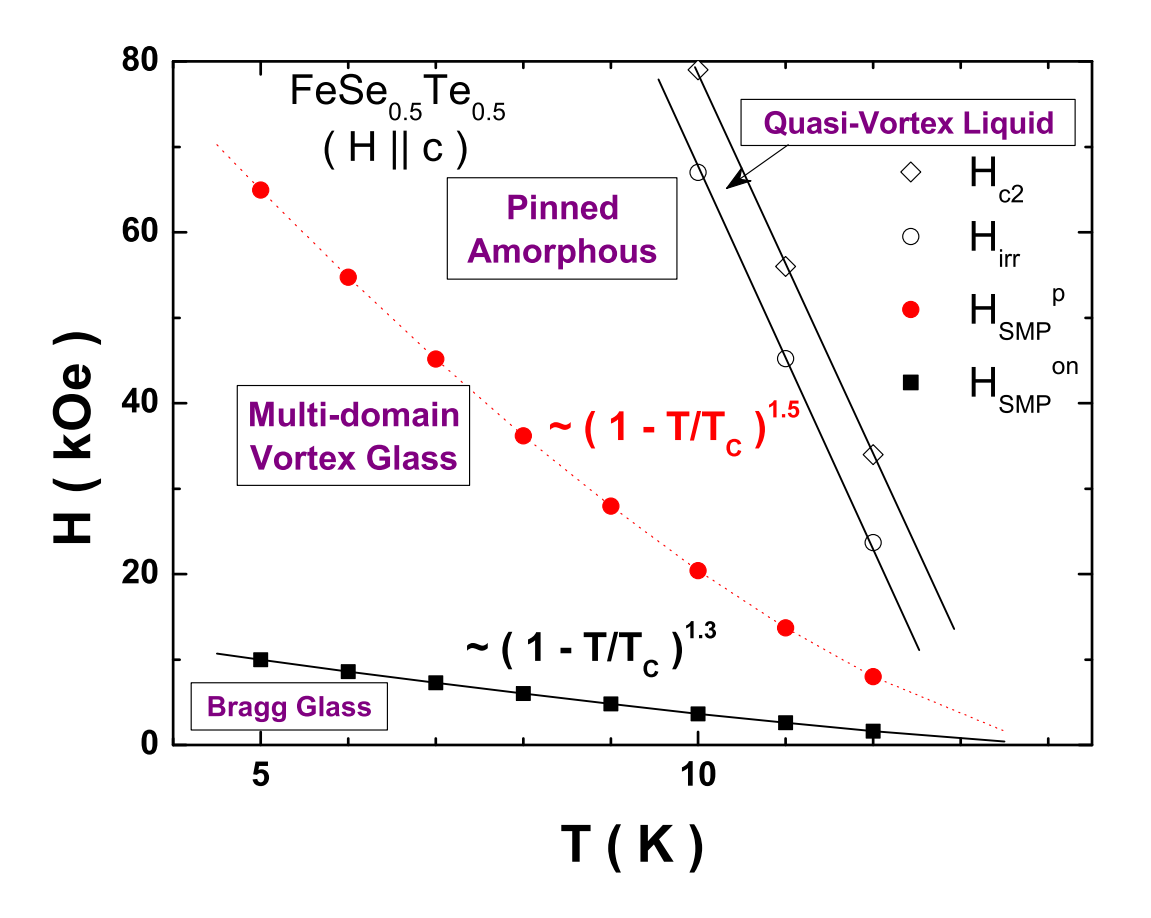


FIG. 6: (Color online) The vortex phase diagram for FeSe<sub>0.50</sub>Te<sub>0.50</sub>.

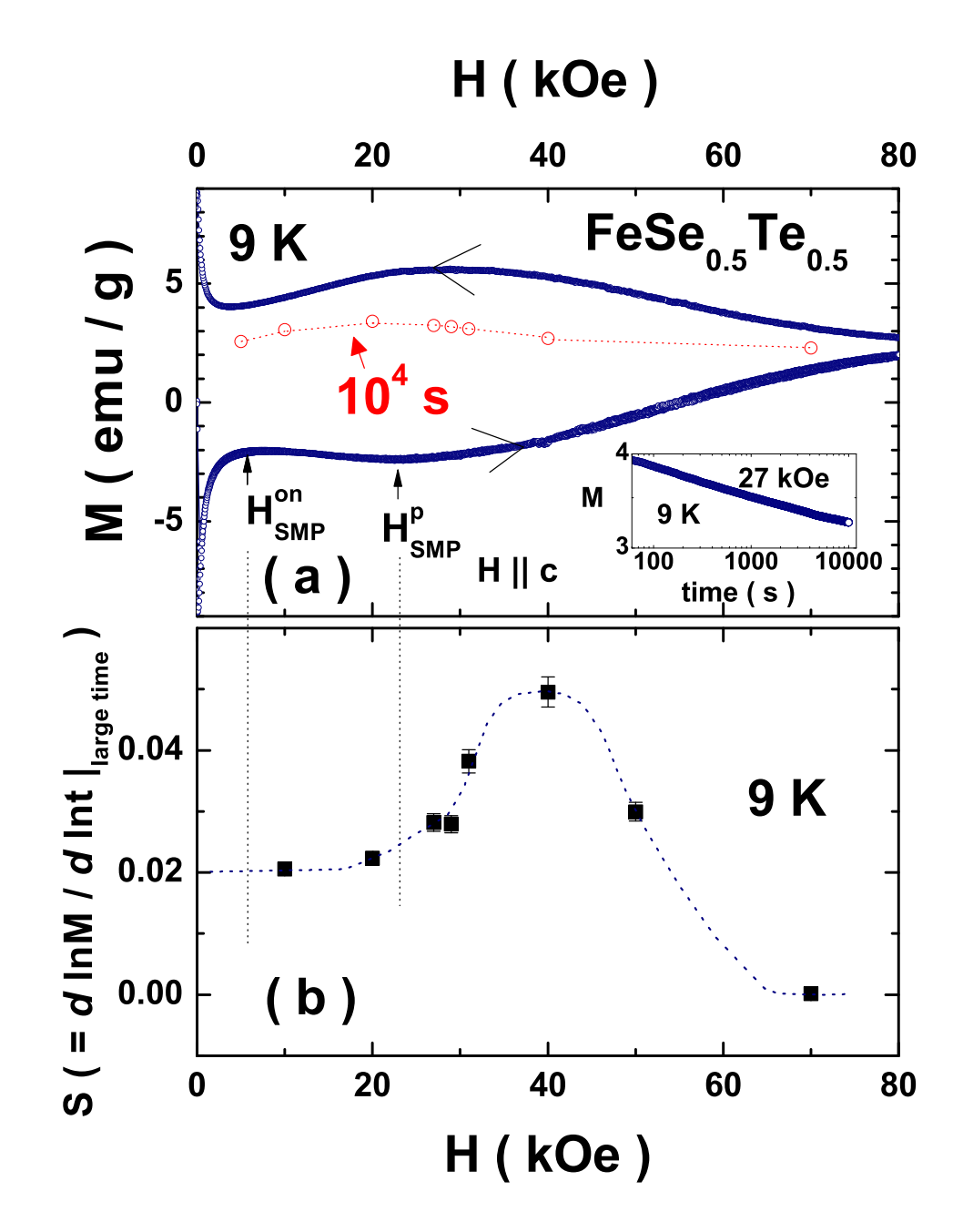


FIG. 7: (Color online) Relaxation across the fishtail effect in FeSe<sub>0.50</sub>Te<sub>0.50</sub>: (a) portion of isothermal M-H loop at 9 K ( $t = \frac{T}{T_c} = 0.63$ ). The inset in panel (a) shows the time decay (M(t)) data measured up to  $10^4$  s at 27 kOe and 9 K. The open red symbols show the magnetization values at  $10^4$  s at respective fields with the dotted line being a guide to eye for the relaxed return leg of the M-H loop at  $10^4$  s, (b) S-parameter as a function of field at 9 K.

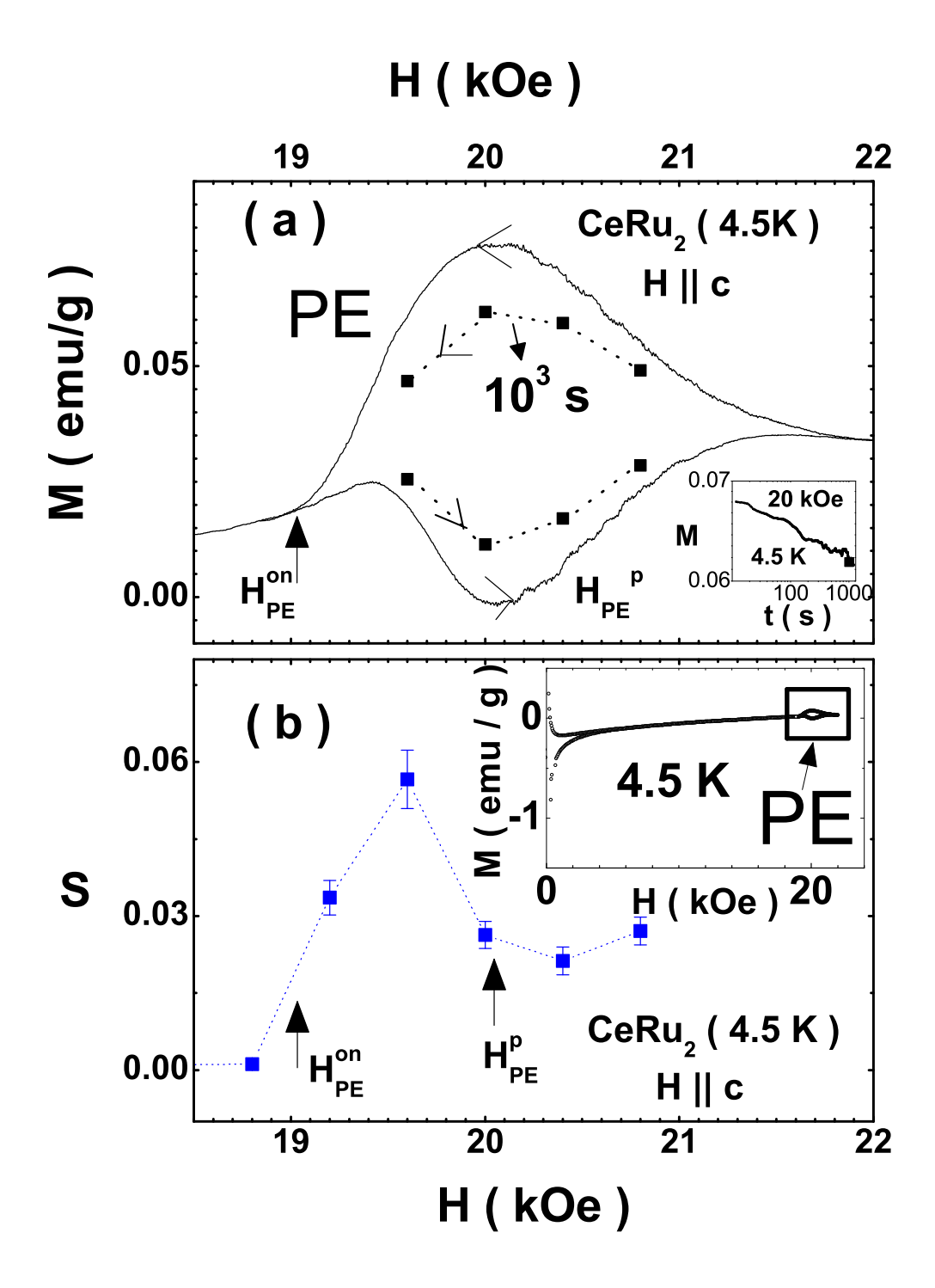


FIG. 8: (Color online) Relaxation data across the Peak Effect (PE) in CeRu<sub>2</sub>: (a) portion of isothermal M-H loop at 4.5 K in the PE region. The inset in panel (a) shows the time decay (M(t)) data measured up to 10<sup>3</sup> s at 20 kOe and 4.5 K, (b) S-parameter as a function of field at 4.5 K. The inset in panel (b) shows the 2 quadrant isothermal M-H loop obtained at 4.5 K with the PE being highlighted by the boxed region.